



Ag/ZnO nanocomposite for effective dye degradation in presence of sunlight and antibacterial activity

Gnanamani Simiyon G & Mary Vergheese T*

Department of Chemistry, Madras Christian College (Affiliated to University of Madras), East Tambaram, Chennai 600 059, India

E-mail: maryvergheese@mcc.edu.in

Received 19 August 2022; accepted 21 October 2022

In recent years search for efficient material to detoxify the environment has received great interest. Nanomaterials made up of transition metal oxide proved to be promising material for future owing to their extraordinary physical, chemical, and electronic properties. Among the different metal oxides, zinc oxide (ZnO) with wide band, good photostability, easy to prepare and low cost make it a viable source to remediate the environment. Addition of plasmonic structure to ZnO inhibits the charge carrier recombination and aids to absorb visible light. In this work, Ag/ZnO nanocomposites have been prepared using thermal method and characterized using X-ray diffraction, diffuse reflectance spectroscopy, scanning electron microscopy and energy dispersive analysis. Photocatalytic studies under sunlight to degrade methylene blue dye indicates the ability of synthesized material that can be utilized to treat dye effluents. The synthesized material has also shown good antibacterial activity.

Keywords: Dye degradation, Environment remediation, Photocatalysis, Plasmonic catalyst

Industrialization has provided comfortable life but has a serious impact on our environment¹. Synthetic dyes makes our world colourful but discharge of residual dye effluents from the various industries without proper treatment pose a serious threat to ground water reserves and aquatic life². Due to their low biodegradability, conventional methods fail to remove the organic pollutants from our environment³. Recently, many methods such as filtration, adsorption, advanced oxidation processes (AOPs) and dendrimer stabilized nanoparticles using engineered nanomaterials to eliminate residual dyes from the environment^{4,6}. AOPs decompose and mineralize organic dye present in dye effluent into eco-friendly compounds and serve as promising tool to remediate our environment^{7,8}. AOPs generate reactive oxygen species (ROS) such as hydroxyl radical (OH[•]) and superoxide radical (O₂^{•-}) with oxidation potential +2.7 eV and -2.3 eV, respectively². Owing to the difference in the oxidation potential of ROS, any organic compound will gain or lose electrons immediately and degrade into small fragments⁹. When compared to conventional chemical treatment, AOPs show effective removal of pollutants by decreasing the chemical oxygen demand (COD) by 90% and removing the color by 95%¹⁰. Among the various AOPs, photocatalytic degradation emerged as better

candidate¹¹⁻¹⁴ due to less energy consumption and utilizes solar energy to effectively convert organic pollutants into water and carbon dioxide. Photocatalysis can be the strategy to remediate the environment by utilizing renewable solar energy¹⁵. A typical photocatalysis process has a photocatalyst which is a semiconductor to absorb photons to create charge separation to initiate redox reaction. In recent years, it is understood that the key steps in photocatalysis are light harvesting, electron – hole pair generation and separation, and catalytic reaction¹⁶. Transition metal oxides (TiO₂, ZnO, Fe₂O₃, Ta₂O₃, CuO, NiO, Cr₂O₃, RuO₂, etc.) with wide band gaps are employed as photocatalysts to remove organic pollutants¹⁷. Among the various heterogeneous photocatalysts, zinc oxide and silver and gold nanoparticles emerged as a more promising candidate for managing the environmental crisis due to pollution¹⁸⁻²¹. Due to high band gap, zinc oxide must be excited with UV irradiation to act as a photocatalyst which consumes high cost and energy. Zinc oxide has low efficiency in charge separation which is yet another reason for poor photocatalytic property²². One of the methods to improve the photocatalytic activity is by introducing heterostructure to inhibit the recombination of charge carrier. Plasmonic metal nanoparticles show visible light absorption and it is

tunable based on the size and structure²³ and with incorporation over a semiconductor, it helps to scatter and trap the light²⁴. Plasmonic structure also aids in the absorption of visible light *via* surface plasmon resonance (SPR)²⁵⁻²⁹. Noble metal nanoparticles have a high energy surface and to minimize the surface energy it undergoes agglomeration or is involved in chemical transformation by absorbing toxic pollutants onto their surface and detoxifying the environment³⁰. Addition of noble metal creates Schottky barriers at the interface and it accelerates electron transport between the interface of noble metal and semiconductor³¹. Methylene blue is basic dye which is commonly used in textiles industries resulting one of the major composition in the dye effluent. Methylene blue is carcinogenic in nature and poses serious threat to marine life and us^{32,33}.

With this background, silver – zinc oxide (Ag/ZnO) nanocomposites have been synthesized using thermal method and characterized using diffuse reflectance spectroscopy (DRS – UV), X-ray diffraction (XRD), scanning electron microscopy (SEM), and energy dispersive analysis (EDX). Photocatalytic ability of Ag/ZnO nanocomposites has been studied using degradation of methylene blue under sunlight. Additional, Ag/ZnO nanocomposites have shown excellent antibacterial activity.

Experimental Section

Chemicals

Zinc sulphate heptahydrate, sodium hydroxide, silver nitrate, ammonia and glucose were purchased from LobaChemie and used without any further purification.

Characterization techniques

The optical property of synthesized material was characterized by diffuse reflectance spectroscopy (UV-DRS) using JASCO V-660 UV-Visible spectrometer and X-Ray diffraction (XRD) using Bruker D8 Powder X-ray diffractometer. Scanning electron microscopy (SU6600, Hitachi) was used to study the surface morphology and elemental composition of the synthesized material.

Preparation of ZnO and Ag/ZnO

Zinc sulphate (0.1 M, 250 mL) was heated to 75°C in a 1 L beaker. To the hot solution freshly prepared mixture of silver nitrate (0.001 M, 0.0025 M, 0.005 M and 0.01 M) solution in alkaline medium and 2g of glucose in water was added at once and stirred

vigorously. Sodium hydroxide (0.2 M, 250 mL) was added dropwise and continuously stirred for 2 h. Resultant precipitate was filtrated, washed and dried at 120°C. Dried precipitate was annealed at 600°C. Final product was Ag/ZnO nanocomposite. Similar method was adapted to prepare ZnO nanomaterial without addition of silver nitrate and glucose mixture.

Photocatalytic studies

The photocatalytic ability of the synthesized Ag/ZnO was studied using methylene blue dye degradation under sunlight. The photocatalytic studies were carried out between 11 am to 2 pm of a day at Madras Christian College with sunlight intensity greater than 10000 lux. In a typical experiment, 0.15 g of synthesized Ag/ZnO was added to 300 mL of 10 ppm solution of methylene dye and was taken in 500 mL beaker and stirred for 2 h under dark before exposure to sun light to establish adsorption-desorption equilibrium between the catalyst surface and dye. Later, the system was exposed to sunlight and degradation process was studied by measuring the absorbance with spectrophotometer at 660 nm.

Antibacterial studies

The study was conducted in a labelled and sterile 96 well plate under aseptic condition. The first row of the plate was filled with 100 µL of test material in 10% (v/v) DMSO. 50 µL of nutrient broth was added to all other wells and serial dilutions were performed. To each well 10 µL of resazurin indicator, 30 µL of nutrient broth, and finally 10 µL of bacterial suspension were added. To avoid dehydration, plates were wrapped loosely with cling film and placed in an incubator at 37°C for 18–24 h. Change in colour from purple to pink indicates the positive response and low concentration at which colour change was recorded as minimum inhibitory concentration (MIC) value.

Results and Discussion

X-ray diffraction studies indicate ZnO displayed hexagonal wurtzite crystal structure without any other crystalline phase¹³. The XRD peaks at 2θ 31.7, 34.5, 36.4, 47.4, 56.5, 62.8, 68.0, and 69.1° were assigned to the (100), (002), (101), (102), (110), (103), (112) and (201) reflection planes of hexagonal ZnO respectively (JCPDS No. 79-2205). Additional peaks in Fig. 1 confirm the addition of silver nanoparticles to zinc oxide. Figure 2 show XRD pattern of pristine ZnO and different composition of Ag/ZnO nanocomposites indicating the formation of pure

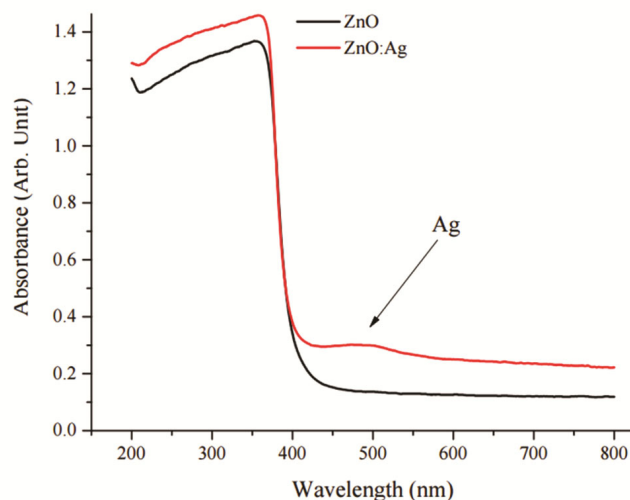


Fig. 1 – UV-DRS spectra of ZnO and Ag/ZnO.

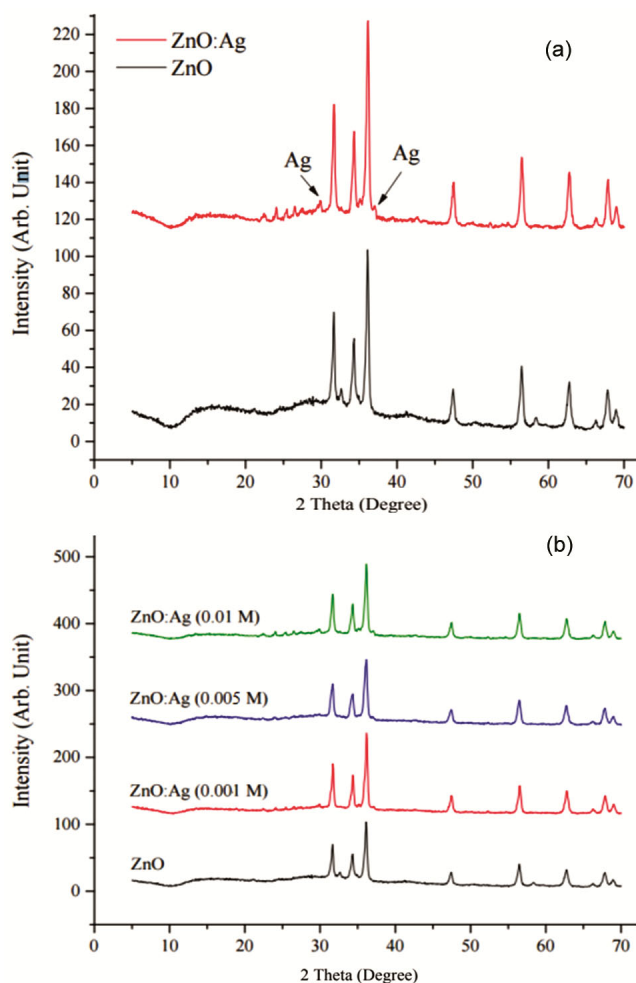


Fig. 2—(a) XRD spectra of ZnO and Ag/ZnO and (b) XRD spectra of pristine ZnO and different composition of Ag/ZnO nanocomposites.

phase of ZnO and addition peaks attributed to addition of silver nanoparticles.

Surface morphology is characterized using scanning electron microscope (SEM). SEM images (Fig. 3) shows the formation of Agglomerated Ag/ZnO nanocomposites showing flakes like structure. The particle size of Ag/ZnO found to be 70 – 85 nm which provide larger surface area to accelerate the degradation process via photocatalysis. The elemental composition of the Ag/ZnO nanocomposites was characterized using energy dispersive X-ray (EDX) analysis indicates the presence and elemental composition ratio of Zinc, oxygen and silver (Fig. 4). This confirms the addition of silver to zinc oxide in Ag/ZnO nanocomposite.

Optical characterization was carried out using diffuse reflectance spectroscopy (DRS). Figure 1 shows the UV-DRS spectra of both ZnO and Ag/ZnO (Zn:Ag = 1:0.01 M) nanomaterials. A small shoulder is observed around 500 nm indicates the addition of plasmonic band due to interaction between semiconductor ZnO and silver nanoparticles. When compared to pristine ZnO, Ag/ZnO absorbs more visible light due to presence of plasmonic band and added silver nanoparticles can act as

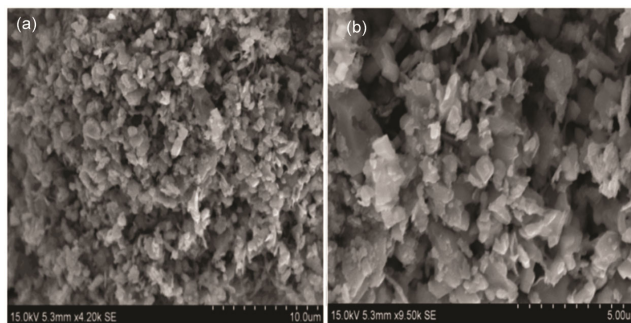


Fig. 3 – SEM Images of Ag/ZnO nanocomposite at magnification of (a) 10 μm and (b) 5 μm.

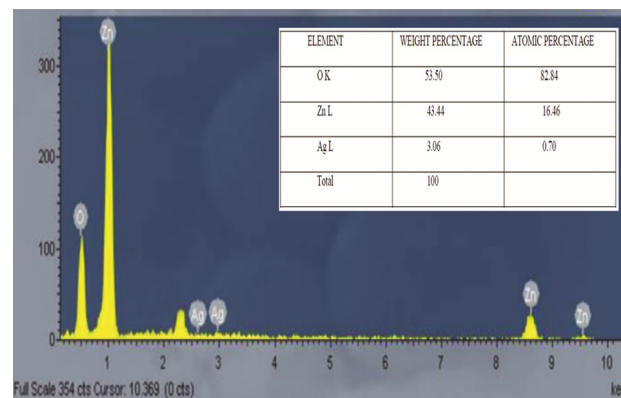


Fig. 4 – EDX spectra and inset showing the elemental composition of Ag/ZnO nanocomposites.

Table 1—Comparison of current study with recent literature.

S No.	Irradiation source	Dye	Time (min)	Degree of degradation (%)	Antibacterial studies	Ref.
1	Visible light	MB	80	90	Yes	34
2	Visible light	MB	30	9	-	35
3	Solar light	CR and MO	80	96 (CR) and 94 (MO)	Yes	36
4	UV-visible light	RhB and MO	35	99.3 (RhB) and 99.7 (MO)	-	37
5	Solar light	MB	45	99	Yes	This work

Methylene Blue (MB), Congo Red (CR), Methyl Orange (MO) and Rhodamine B (RhB)

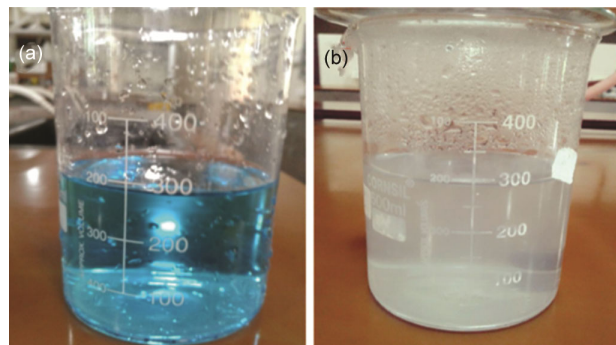


Fig. 5—Methylene blue dye (10 ppm) solution under sunlight (a) before and (b) after exposure.

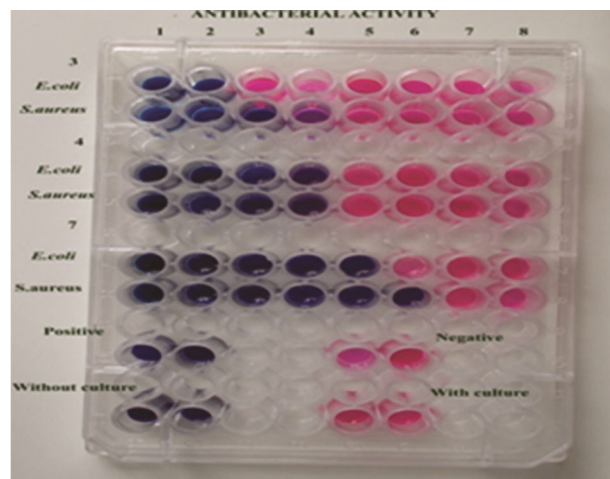


Fig. 6—Colour change from pink to purple which infers the antibacterial effect.

electron sink to promote better charge carrier stability and photocatalytic property of the material.

Photocatalytic studies

The photocatalytic property of ZnO nanomaterial and Ag/ZnO nanocomposites (Zn: Cu ratio is 1:0.01) were studied by the degradation of methylene blue dye under sunlight. Pristine ZnO failed to degrade methylene blue under sunlight whereas Ag/ZnO nanocomposite exhibited excellent photocatalytic activity degrading methylene blue under sunlight as shown in Fig. 5.

This is due to (i) addition of plasmonic band of silver nanoparticles aids the Ag/ZnO to absorb more

Table 2—MIC values for pure and Ag/ZnO nanocomposites.

Microorganisms	MIC value (mg)
ZnO	
<i>E. Coli</i>	2.5
<i>S. Auerus</i>	0.625
Ag/ZnO (1:0.005)	
<i>E. Coli</i>	0.625
<i>S. Auerus</i>	0.625
Ag/ZnO (1:0.01)	
<i>E. Coli</i>	0.312
<i>S. Auerus</i>	0.156

visible light (ii) energy gap between Fermi levels of silver and zinc oxide is small and Schottky barrier formed between the silver nanoparticles and zinc oxide semiconductor provides medium for faster electron transport (iii) silver nanoparticles acts as electron sink this provide longer lifetime for the electron – hole pair separation or charge carrier. Decolouration indicates the degradation of dye and time taken for complete degradation of dye sample was 45 min.

From the results, it is evident that addition of silver to ZnO aids catalyst to absorb and utilize the visible light efficiently than pristine ZnO. From Table 1, Ag/ZnO nanocomposites harvest renewable solar energy and efficiently degrade which make it prominent material to degrade pollutants. The catalyst is recycled by filtering after photocatalytic studies and drying. Similar experiments were carried out for five times, the recycled Ag/ZnO photocatalyst exhibited similar degradation ability proving the material as viable alternative to remediate our environment.

Antibacterial studies

Antibacterial testing was carried out for a gram-positive and gram-negative bacteria (Fig. 6). The minimum inhibitory concentration was determined. The minimum inhibitory concentration (MIC) is the lowest concentration of material, which inhibits the growth of an organism. It was determined on cultures containing different concentration of stock solution containing pure ZnO and Ag/ZnO nanocomposites. MIC for Ag/ZnO is found to 0.31 mg (*E. Coli*) and 0.16 mg (*S. Auerus*) (Table 2).

Conclusion

ZnO and Ag/ZnO have been successfully prepared via thermal method. UV – DRS spectra indicates the addition on plasmonic band due to presence of silver in the ZnO. From SEM analysis, flake morphology has been observed with particle size 70 – 85 nm. Addition of silver to zinc oxide, enhanced the light absorption capacity and photocatalytic ability of the nanocomposites. With enhanced photocatalytic property, Ag/ZnO nanocomposite degrades methylene blue dye completely in 45 min under sunlight and also recyclable proving it a prominent material to remediate our environment. Addition of silver to zinc oxide also increases the antibacterial property of the nanocomposites adds more value to synthesized material.

Acknowledgement

The authors thank Mrs. Maria Sangeetha, Ms. Neelu Mariam Varghese, Ms. Nivetha Basavaraj for their support in presenting this work. The authors also thank Department of Chemistry, Madras Christian College for providing facility to carry out this work.

Reference

- Nie M, Liao J, Cai H, Sun H, Xue Z, Guo P & Wu M, *Chem Phys Lett*, 768 (2021) 138394.
- Anwer H, Mahmood A, Lee J, Kim K H, Park J W & Yip A C, *Nano Res*, 12 (2019) 955.
- Montoya-Rodríguez D M, Serna-Galvis E A, Ferraro F & Torres-Palma R A, *J Environ Manage*, 261 (2020) 110224.
- Samadi M, Zirak M, Naseri A, Kheirabadi M, Ebrahimi M & Moshfegh A Z, *Res Chem Intermed*, 45 (2019) 2197.
- Murugan E & Pakrudheen I, *Appl Catal A: General*, 439 (2012) 142.
- Murugan E, Jebaranjitham J N, Raman K J, Mandal A, Geethalakshmi D, Dharmendra Kumar M & Saravanakumar A, *New J Chem*, 41 (19) 10860.
- Mauter M S, Zucker I, Perreault F, Werber J R, Kim J H & Elimelech M, *Nat Sustain*, 1 (2018) 166.
- Zhao L, Denga J, Sun P, Liu J, Ji Y, Nakada N, Qiao Z, Tanaka H & Yang Y, *Sci Total Environ*, 627 (2018) 1253.
- Weinberg N L & Weinberg H R, *Chem Rev*, 68 (1968) 449.
- Azbar N U R I, Yonar T & Kestioglu K, *Chemosphere*, 55 (2004) 35.
- Lee K M, Lai C W, Ngai K S & Juan J C, *Water Res*, 88 (2016) 428.
- Ratnayake S P, Mantilaka M M M G P G, Sandaruwan C, Dahanayake D, Murugan E, Santhosh Kumar S, Amaratunga G A J & Nalin de Silva K M, *Appl Catal A: Gen*, 570 (2019) 23.
- Murugan E & Rangasamy R, *J Biomed Nanotechnol*, 7 (2011) 225.
- Murugan E & Shanmugam P, *Bull Mater Sci*, 38 (2015) 629.
- Kudo A & Miseki Y, *Chem Soc Rev*, 38 (2009) 253.
- Li Y, Gao C, Long R & Xiong Y, *Mater Today Chem*, 11 (2019) 197.
- Danish M S S, Estrella L L, Alemaida I M A, Lisin A, Moiseev N, Ahmadi M, Nazari M, Wali M, Zaheb H & Senju T, *Metals*, 11 (2021) 80.
- Prasad V, Gnanamani Simiyon G, Ansha E M & Jayaprakash N, *Rasayan J Chem*, 12 (2019) 860.
- Lee K M, Lai C W, Ngai K S & Juan J C, *Water Res*, 88 (2016) 428.
- Murugan E & Shanmugam P, *J Nanosci Nanotechnol*, 16 (2016) 426.
- Murugan E & Jebaranjitham J N, *J Biomed Nanotechnol*, 7 (2011) 158.
- Ong C B, Ng L Y & Mohammad A W, *Renew Sustain Energy Rev*, 81 (2018) 536.
- Cushing S K & Wu N, *J Phys Chem Lett*, 7 (2016) 666.
- Wu N, *Nanoscale*, 10 (2018) 2679.
- Li R, Li T & Zhou Q, *Catalysts*, 10 (2020) 804.
- Yogaraj V, Gowtham G, Akshata C R, Manikandan R, Murugan E & Arumugam M, *J Drug Deliv Sci Technol*, 58 (2020) 101785.
- Murugan E, Santhosh Kumar S, Reshna K M & Govindaraju S, *J Mater Sci*, 54 (2019) 5294.
- Santhoshkumar S & Murugan E, *Appl Surf Sci*, 553 (2021) 149544.
- Santhoshkumar S & Murugan E, *Dalt Trans*, 50 (2021) 17988.
- Gopakumar D A, Pai A R, Pasquini D, Ben L S Y, Khalil H P S A & Thomas S, *Nanoscale Mater Water Purif*, (2019) 1.
- Wanga Z, Ye X, Chen L, Huang P, Wang Q, Ma L, Hua N, Liu X, Xiao X & Chen S, *Mater Sci Semicond Process*, 121 (2021) 105354.
- Murugan E, Akshata C R, Yogaraj V, Sudhandiran G & Babu D, *Ceram Int*, 48 (2022) 16000.
- Mahmoud M S, Farah J Y & Farrag T E, *J Pet*, 22 (2013) 211.
- Ziashahabi A, Mirko P, Zhiya D, Reza P & Naimeh N, *Sci Rep*, 9 (2019) 1.
- Khan M J, *Photodiagnosis Photodyn Ther*, 36(2021) 102619.
- Chauhan A, *Sci Rep*, 10 (2020) 1.
- Lim H, Mohammad Y, Sehwan S, Sungkyun P & Kang H P, *RSC Adv*, 11 (2021) 8709.